Seismic Response Analysis with Spatially Varying Stochastic Excitation

Katerina Konakli

Abstract Assessment of the seismic vulnerability of extended structures (e.g. bridges and lifelines) as well as of systems of structures covering extended areas requires to properly account for the effects of ground-motion spatial variability. Even in cases with relatively uniform soil conditions, ground motions may exhibit significant variations due to the incoherence and wave-passage effects, respectively manifested as random differences and deterministic time delays. Differential soil conditions cause additional variations in the amplitude and frequency content of the ground motions as these propagate from the bedrock to the surface level. The present chapter describes methods for the modeling of ground-motion spatial variability, the simulation of spatially varying ground-motion arrays and the evaluation of the response of multiply-supported structures to differential support excitations. The pertinent uncertainties in the characteristics of the ground motions are accounted for by employing concepts from stochastic time-series analysis. In particular, the notion of coherency is employed to describe the spatial variability of the ground-motion arrays, which are considered as realizations of a random field at the locations of interest. The statistical properties of the ground motions at separate locations are described through the respective auto-power spectral densities. A statistical characterization of linear structural response to differential support motions is obtained by means of a response-spectrum method, rooted in random vibration theory, while the non-linear response is investigated on the basis of the 'equal-displacement' rule. This chapter is inspired by the doctoral research of the author under the supervision of Professor Armen Der Kiureghian.

K. Konakli (✉)
ETH Zürich, Chair of Risk, Safety and Uncertainty Quantification,
Stefano-Franscini-Platz 5, HIL E23.2, 8093 Zürich, Switzerland
e-mail: konakli@ibk.baug.ethz.ch

P. Gardoni (ed.), *Risk and Reliability Analysis: Theory and Applications*,
Springer Series in Reliability Engineering, DOI 10.1007/978-3-319-52425-2_9

1 Introduction

Several recent earthquake events across the globe highlight the need for improved measures to safeguard people's lives and properties in seismic vulnerable areas. The immense uncertainties associated with the occurrence and the characteristics of future ground motions pose a major challenge in dealing with seismic risk. The work of Professor Armen Der Kiureghian has been fundamental in achieving this goal by offering pioneering methods for addressing uncertainty in the field of earthquake engineering, among his numerous valuable contributions in the broader fields of risk and reliability (e.g. Der Kiureghian and Liu 1986; Der Kiureghian and Ke 1988; Der Kiureghian et al. 1994; Song and Der Kiureghian 2003; Straub and Der Kiureghian 2010).

Inspired by the doctoral work of the author under the supervision of Professor Der Kiureghian, the present chapter focuses on a particular aspect of seismic analysis that is the spatial variability exhibited by earthquake-induced ground motions and its effects on structural response. The importance of incorporating these effects in seismic response analysis arises from the fact that seismic ground motions may exhibit significant variations over distances that are comparable to the dimensions of extended structures, such as bridges and lifelines. Furthermore, the ground-motion spatial variability comes into play when examining seismic vulnerability at a systemic level, considering the infrastructure of entire communities rather than independent structures. It should be emphasized that awareness on the need for a systemic perspective is currently growing in the engineering research community.

This chapter provides an overview on the following topics: the modeling of ground-motion spatial variability, the simulation of spatially varying ground-motion arrays and the response analysis of extended structures subject to differential support excitations. In the relevant methods presented herein, effects of uncertainties are incorporated by considering the ground-motion time histories as realizations of stochastic processes exhibiting spatial correlations. To this end, mathematical tools for time-series analysis in both the time and frequency domains are employed.

Following the Introduction, the coherency function is presented in the next section, as a means of describing the spatial variability of stochastic processes in the frequency domain. Moreover, popular models for the coherency function in the field of earthquake engineering are described. The section continues with the estimation of coherency from ground-motion records, including a case study using accelerograms from the 2004 Parkfield earthquake in California.

The subsequent section describes a method for simulating ensembles of spatially varying ground-motion arrays consistent with a prescribed coherency function. It is underlined that because recorded strong ground-motion arrays remain scarce, methods for generating such arrays synthetically are essential in earthquake engineering research and practice. The method described herein relies on the theory of Gaussian random processes. Two approaches are presented: in the so-called

unconditioned approach, the power spectral density of the acceleration process at a reference site is defined on the basis of a given recorded or synthetic accelerogram. In this case, ensembles of simulated arrays exhibit uniform variability at different locations, a necessary property when these motions are used as input for statistical analyses of structural responses. In the second approach, a specific realization (a recorded or synthetic accelerogram) at a reference site is defined and consistent time histories are simulated at the locations of interest. The latter comprises the conditioned approach.

In the next part of this chapter, the focus is set on methods for the evaluation of structural response to differential support excitations. First, a response-spectrum method is described, rooted in the theory of random vibrations. This method is well known as the Multiple-Support Response-Spectrum (MSRS) rule. Developed by Der Kiureghian and Neuenhofer (1992), the MSRS rule is nowadays incorporated in seismic design codes. The extension of the MSRS rule to account for quasi-static contributions of truncated high-frequency vibration modes, developed by Konakli and Der Kiureghian (2011a), is also presented. In the sequel, effects of spatial variability on the 'equal-displacement' rule, relating mean peak non-linear to mean peak linear structural responses, are discussed.

A summary is included in the final section of this chapter, followed by a grateful acknowledgement to Professor Der Kiureghian.

2 Modeling of Ground-Motion Spatial Variability

2.1 The Coherency Function

The spatial variability manifested in earthquake-induced ground motions can be attributed to three main effects, namely the incoherence, the wave-passage and the site-response effects (Der Kiureghian 1996). The incoherence effect represents random differences in the amplitudes and phases of seismic waves due to reflections and refractions that occur as the waves propagate in the heterogeneous soil medium and also, due to the super-positioning of waves arriving from different parts of an extended source. The wave-passage effect represents the deterministic time-lag that characterizes the arrival of seismic waves at separate locations. The site-response effect represents the influence of varying local soil profiles on the amplitude and frequency content of the bedrock motions as they propagate upwards to the surface. The aforementioned effects are incorporated into the complex-valued coherency function, which models the ground-motion spatial variability in the frequency domain. Details on the coherency function are given in the sequel.

Let $\ddot{u}_k(t)$ and $\ddot{u}_l(t)$ denote a pair of stationary random processes modeling the ground-motion accelerations at locations k and l respectively. The coherency function that characterizes the spatial variability between the two locations is a normalized version of the cross-power spectral density (PSD) of $\ddot{u}_k(t)$ and $\ddot{u}_l(t)$:

$$\gamma_{kl}(\omega) = \frac{G_{\ddot{u}_k\ddot{u}_l}(\omega)}{\left[G_{\ddot{u}_k\ddot{u}_k}(\omega)G_{\ddot{u}_l\ddot{u}_l}(\omega)\right]^{1/2}}. \quad (1)$$

where $G_{xy}(\omega)$ denotes the cross-PSD of the random processes $x(t)$ and $y(t)$, and $G_{xx}(\omega)$ denotes the auto-PSD of process $x(t)$. Although earthquake ground motions are not stationary, the above definition of the coherency function is commonly used to describe their spatial variability under the assumption that the strong-motion phase of an accelerogram is nearly stationary.

In the case of uniform soil conditions, the modulus of the coherency function characterizes the incoherence effect, whereas its phase angle characterizes the wave-passage effect. Der Kiureghian (1996) has shown that, under the assumption of vertical wave propagation from the bedrock level to the ground surface, the site-response effect influences only the phase angle of the coherency function. This assumption can be employed in the case of far-field earthquake records. In this case, the coherency function can be written in the form:

$$\gamma_{kl}(\omega) = |\gamma_{kl}(\omega)| exp\left\{i[\theta_{kl}^{wp}(\omega) + \theta_{kl}^{sr}(\omega)]\right\} \quad (2)$$

where $\theta_{kl}^{wp}(\omega)$ and $\theta_{kl}^{sr}(\omega)$ respectively denote the phase angles due to wave-passage and site-response effects. It is noted that in the case of near-fault motions, site-response effects may also influence the coherency modulus.

Based on the physics of wave propagation and certain simplifying assumptions, it is possible to develop theoretical models to describe the phase angle caused by the wave-passage and site-response effects (the latter for far-field sites). The phase angle due to the wave-passage effect is typically evaluated as (Luco and Wong 1986; Der Kiureghian 1996):

$$\theta_{kl}^{wp}(\omega) = -\frac{\omega d_{kl}^{L}}{\nu_{app}} \quad (3)$$

where d_{kl}^{L} is the projected algebraic horizontal distance in the longitudinal direction of propagation of waves and ν_{app} is the surface apparent wave velocity. Under the assumptions of linear (or linearized) behavior of the soil columns, vertical wave propagation at each site and neglect of dynamic interaction between sites, the phase shift due to the site-response effect is given by (Der Kiureghian 1996):

$$\theta_{kl}^{sr}(\omega) = tan^{-1}\frac{Im[H_k(\omega)H_l(-\omega)]}{Re[H_k(\omega)H_l(-\omega)]} \quad (4)$$

where $H_k(\omega)$ is the frequency-response function for the absolute acceleration response of the soil column at location k.

The inherently random nature of the incoherence effect renders the description of the coherency modulus more challenging. One approach is to use a semi-empirical

model, i.e. a theoretical model employing parameters that can be determined through statistical inference. Another approach is to develop a purely empirical model using data from recorded acceleration arrays. Empirical models account for the complex phenomena that occur during wave propagation and are not captured by simplified mathematical models, but characterize only the specific rupture mechanisms and soil topographies present in the data. Among the most quoted empirical models are those by Harichandran and Vanmarcke (1986) and Abrahamson et al. (1991), which are based on ground motions recorded by two arrays located in an alluvial valley in Taiwan. Ancheta et al. (2011) updated the coefficients of the latter so that the new model additionally fits data from the Borrego Valley Differential Array in California.

One of the most widely used semi-empirical models in engineering applications was derived by Luco and Wong (1986) considering the propagation of shear waves in a random medium. According to this model, the coherency modulus for a pair of acceleration processes at stations k and l separated by a distance d_{kl} is evaluated as:

$$|\gamma_{kl}| = exp\left[-(\alpha d_{kl}\omega)^2\right] \tag{5}$$

in which the coherency drop parameter α is given by $\alpha = \eta/v_s$, where v_s is the average shear-wave velocity of the ground medium along the wave travel-path and η is a constant. Luco and Wong suggested that typical values of α approximately vary from 2×10^{-4} to 3×10^{-4} s/m, whereas Zerva and Harada (1994) proposed an analytical expression for α in terms of the properties and depth of the soil layers at the site under consideration. The Luco and Wong model represents a special case of the model developed by Der Kiureghian (1996) based on the theory of random processes.

2.2 Estimation of the Coherency Modulus

Consider an array of zero-mean, jointly stationary Gaussian ground-acceleration processes at n sites defined by auto-PSDs $G_{kk}(\omega)$, $k = 1, 2, \ldots, n$, and cross-PSDs $G_{kl}(\omega)$, $k, l = 1, 2, \ldots, n$, for $k \neq l$. Let $a_k(t_i)$ and $a_l(t_i)$, $i = 1, \ldots, N$, represent realizations of the acceleration processes at locations k and l respectively, each sampled at equal time intervals Δt, i.e. $t_i = (i-1)\Delta t$. To simplify the algebra, N is considered even. According to Eq. 1, estimation of the coherency function from given realizations requires the respective auto- and cross-PSDs. Under the assumption of ergodicity, these quantities can be estimated from a single realization of a random field, as described below.

An estimator of the auto-PSD of the acceleration record at location k is the periodogram:

$$I_{kk}(\omega_p) = (N\Delta t/4\pi)\left(A_{pk}^2 + B_{pk}^2\right) \tag{6}$$

in which $\omega_p = 2\pi p/N\Delta t$, $p = 1, \ldots, N/2 - 1$, denote discrete frequencies and $\{A_{pk}, B_{pk}\}$ are the Fourier coefficients of the acceleration record (Chatfield 2004). Though asymptotically unbiased, the periodogram is an inconsistent estimator and exhibits erratic behavior. The traditional method to obtain a consistent estimator is to smooth the periodogram over a frequency band (Brillinger 2001). The resulting estimates of the PSD depend on the selected width of the smoothing window and, to a lesser extent, on the type of smoother (Priestley 1981). Because smoothing introduces bias to the estimates, the width of the smoothing window should be selected considering the tradeoff between bias and variance.

A consistent estimator of the cross-PSD of two acceleration records is the smoothed cross-periodogram. The real and imaginary parts of the cross-periodogram are respectively determined by Chatfield (2004):

$$Re\left[I_{kl}(\omega_p)\right] = (N\Delta t/4\pi)\left(A_{pk}A_{pl} + B_{pk}B_{pl}\right) \tag{7}$$

and:

$$Im\left[I_{kl}(\omega_p)\right] = (N\Delta t/4\pi)\left(A_{pk}B_{pl} - A_{pl}B_{pk}\right) \tag{8}$$

Finally, an estimate of the coherency function is obtained by substituting in Eq. 1 the smoothed version of $I_{kl}(\omega)$ in the place of $G_{kl}(\omega)$ and the smoothed versions of $I_{kk}(\omega)$ and $I_{ll}(\omega)$ in the places of $G_{kk}(\omega)$ and $G_{ll}(\omega)$ respectively. To estimate the coherency modulus for a pair of accelerograms at sites k and l, the real and imaginary parts of the coherency function are substituted into the expression $|\gamma_{kl}(\omega)| = \left\{[Re(\gamma_{kl}(\omega))]^2 + [Im(\gamma_{kl}(\omega))]^2\right\}^{1/2}$.

2.3 The Case of the UPSAR Array

Recordings of the UPSAR array during the 2004 Parkfield earthquake in California provided a rare opportunity to examine the coherency function for near-fault strong ground motions. Konakli et al. (2014) investigated the coherency modulus for this particular event and tectonic setting and compared their estimates with commonly used semi-empirical and empirical models. This subsection provides a summary of the analysis and main findings of this study.

The coherency analysis in Konakli et al. (2014) was based on the acceleration time-histories recorded at the 12 operational stations of the UPSAR array. By focusing on inter-station distances 0–500 m, the analysis considered 47 station pairs. Estimates of the coherency modulus were obtained for each station pair and for each of the EW, NS (two horizontal) and UD (vertical) components, by

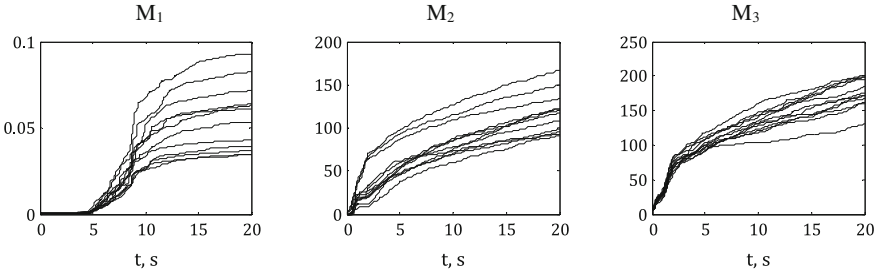

Fig. 1 Evolving measures of variance, predominant frequency and bandwidth of the UPSAR accelerograms in the EW direction

analyzing nearly-stationary segments of the recorded accelerograms. The considered segments were defined by a time window of 7.5 s width, containing the strongest shaking. The selection of the time window was based on an analysis of the following three measures: the integral of the squared acceleration in time (M_1), the cumulative count of zero-level up-crossings (M_2), and the cumulative count of negative maxima and positive minima (M_3). Figure 1 (originally presented in Konakli et al. 2014) shows the time evolution of the aforementioned measures for the accelerograms in the EW direction. Approximately constant slopes of the M_1, M_2 and M_3 curves respectively indicate nearly-constant variance, predominant frequency and bandwidth (Rezaeian and Der Kiureghian 2008). The resulting periodograms for the so selected segments were smoothed using a 5-point Hamming window. Details on the selection of the smoothing window can be found in Konakli et al. (2014).

In order to compare the coherency estimates from the UPSAR recordings to the model by Luco and Wong, values of parameter α in Eq. 5 that fit the UPSAR estimates were determined by means of non-linear least-squares minimization. In examining the coherency at specific distances as a function of frequency, the least-squares minimization was applied on the variance-stabilizing transformation $\tanh^{-1}|\gamma_{kl}|$ (Abrahamson et al. 1991; Ancheta et al. 2011). Figure 2 (originally presented in Konakli et al. 2014) shows the fitter values versus inter-station distances for pairs of components in the NS, EW and UD directions. The figure indicates a strong dependence of α on distance, with α tending to decrease with increasing inter-station distance at a rate that is higher at smaller distances. Overall, the fitted α values for the vertical component are slightly larger than those for the two horizontal components, which tend to be close to each other. This indicates a slightly larger spatial variability among the vertical components than among the horizontal components for the same inter-station distance. The estimated standard deviations of the fitted α values normalized with the respective α values were below 0.2 in all cases.

It is noted that under the assumption of homogeneity, a single estimate of the coherency modulus can be obtained for a relatively narrow inter-station distance bin through averaging. Moreover, under the assumption of isotropy, a single estimate

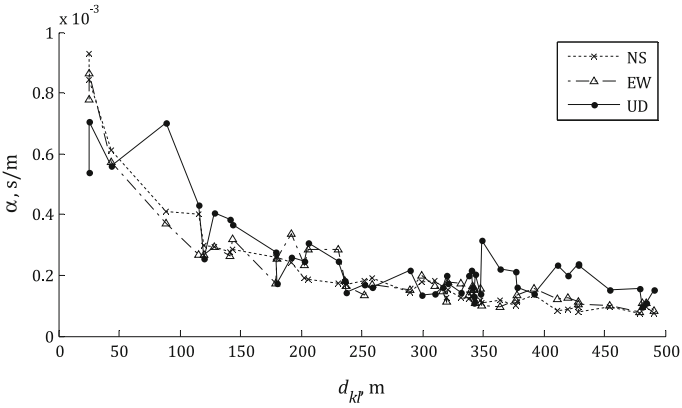

Fig. 2 Fitted α values versus distance using coherency estimates as a function of frequency

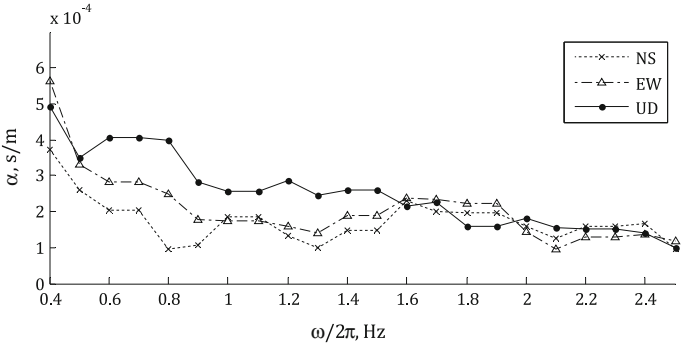

Fig. 3 Fitted α values versus frequency using coherency estimates as a function of distance

can be obtained for the horizontal component of the ground motion. This averaging is important in reducing the noise in the estimates. Fitted α values under the assumptions of homogeneity and isotropy are reported in Konakli et al. (2014).

Next, the behavior of the coherency modulus as a function of inter-station distance is examined at specific frequencies. In this case, the non-linear least-squares minimization is directly applied on $|\gamma_{kl}|$. Figure 3 (originally presented in Konakli et al. 2014) shows the α values obtained for each of the NS, EW and UD components. Frequencies up to 2.5 Hz are shown, because coherency estimates for higher frequencies are dominated by noise. Considering the frequency range below 1.5 Hz, where the effect of noise is relatively small, the figure indicates both direction dependence, with smaller values of α corresponding to the horizontal components, and frequency dependence, with values of α tending to decrease with increasing frequency. The respective estimates of the standard deviation normalized with the fitted α value were below 0.14 in all cases.

According to Figs. 2 and 3, the estimates of α for the UPSAR recordings are within the range suggested by Luco and Wong for distances approximately in the range 100–300 m and for frequencies approximately in the range 0.5–2 Hz. However, unlike the Luco and Wong model where α is a constant, the UPSAR data indicate dependence of α on both inter-station distance and frequency. It is also noted that the rate of decay of the coherency modulus with frequency and distance tends to be higher for the vertical component. This trend is more pronounced for the rate of decay of the coherency modulus with distance at the lower frequencies.

Konakli et al. (2014) further compared estimates of the coherency modulus from the UPSAR recordings with two widely used empirical models. They considered the empirical model by Ancheta et al. (2011) for inter-station distances smaller than 100 m and the model by Harichandran and Vanmarcke (1986) for inter-station distances larger than 100 m. As mentioned earlier in this section, the model by Ancheta et al. (2011) is an update on the earlier model by Abrahamson et al. (1991). For separation distances 100–300 m, the empirical model was found to be in fair agreement with the UPSAR estimates for frequencies up to approximately 4 Hz. For smaller separation distances, the UPSAR coherency modulus was found smaller than that given by the empirical model in the entire frequency range examined, but the trend reversed for separation distances greater than 300 m. These differences indicated a complex dependence of the spatial variability exhibited by earthquake ground motions on source, propagation, topography and site effects.

3 Simulation of Spatially Varying Ground Motions

3.1 The Unconditioned and Conditioned Approaches

The simulation method described in the present section, originally proposed by Konakli and Der Kiureghian (2012a), generates arrays of ground-motion time histories with temporal and spectral non-stationarity, incorporating effects of incoherence, wave passage and differential site response. The method is based on the representation of ground accelerations as realizations of Gaussian random processes and builds upon the earlier works of Vanmarcke and Fenton (1991), Kameda and Morikawa (1992) and Liao and Zerva (2006). The required input comprises: (i) a recorded or synthetic accelerogram at a reference site, (ii) a coherency function that describes the spatial variability of the ground-motion random field and (iii) the frequency-response functions of the soil columns at the locations of interest.

Two approaches are considered. In the unconditioned approach, the simulated motions are consistent with the statistical characteristics of the ground-motion random field at the reference site, derived from the auto-PSD of the given accelerogram. In the conditioned approach, the simulated motions are consistent with the specific realization of the ground-motion random field at the reference site,

represented by the given accelerogram. In the latter approach, the variance of the simulated motions increases with increasing distance from the reference site, which is an undesirable property if the motions are used to perform statistical analysis of structural responses. The unconditioned approach should thus be considered when uniform variance of the simulated motions at different locations is essential.

In both approaches, temporal and spectral non-stationarities are accounted for by considering nearly stationary segments of the given accelerogram. These are used to simulate consistent segments of acceleration time-histories at the target locations, which are appropriately stitched together in the sequel. It is underlined that this method is not directly applicable to near-fault ground motions that contain directivity pulses and thus, cannot be represented as stationary segments even in approximation. One way to include the directivity pulse is to separately model the pulse and superimpose it on a synthetic ground-motion array, the latter generated according to the methodology presented herein.

In the following, after a brief description of the discrete representation of an array of Gaussian processes, the conditioned and unconditioned simulation approaches are outlined for the case of stationary motions. The extension to non-stationary motions is explained in the sequel, followed by an example application.

3.2 Discrete Representation of an Array of Gaussian Processes

Similarly to the previous section, an array of zero-mean, jointly stationary Gaussian acceleration processes at n sites is considered, defined by auto-PSDs $G_{kk}(\omega)$, $k=1,2,\ldots,n$, and cross-PSDs $G_{kl}(\omega)$, $k,l=1,2,\ldots,n$, for $k\neq l$. Each process is sampled at time instants $t_i=(i-1)\Delta t$, $i=1,\ldots,N$, with the number of samples N considered even. Such an array of processes can be represented in terms of the finite Fourier series (see, e.g. Chatfield 2004):

$$a_k(t_i)=A_{0k}+\sum_{p=1}^{N/2-1}\left[A_{pk}\cos\left(\omega_p t_i\right)+B_{pk}\sin\left(\omega_p t_i\right)\right]+(-1)^i A_{(N/2)k} \qquad (9)$$

where $\omega_p=2\pi p/N\Delta t$ are discrete frequencies and $\{A_{pk},B_{pk}\}$ are the Fourier coefficients. Note that the above representation uses N parameters to describe N observations and can thus be made to exactly fit the given realizations.

The Fourier coefficients $\{A_{pk},B_{pk}\}$ are zero-mean, jointly Gaussian random variables, uncorrelated for different frequencies, i.e. $\mathrm{E}[A_{pk}A_{qk}]=\mathrm{E}[B_{pk}B_{qk}]=\mathrm{E}[A_{pk}B_{qk}]=0$ for $p\neq q$. At frequency ω_p, the following relations hold:

$$E\left[A_{pk}\,A_{pl}\right] = E\left[B_{pk}\,B_{pl}\right] = \begin{cases} G_{kk}\left(\omega_p\right)\Delta\omega, & \text{if } k = l \\ Re\left[G_{kl}\left(\omega_p\right)\right]\Delta\omega, & \text{if } k \neq l \end{cases} \tag{10}$$

and

$$E\left[A_{pk}\,B_{pl}\right] = \; -E\left[B_{pk}\,A_{pl}\right] = \begin{cases} 0, & \text{if } k = l \\ Im\left[G_{kl}\left(\omega_p\right)\right]\Delta\omega, & \text{if } k \neq l \end{cases} \tag{11}$$

with $\Delta\omega = 2\pi/N\Delta t$. Obviously, given the auto- and cross-PSDs (or equivalently the auto-PSDs and the coherency function), the variance/covariances of all Fourier coefficients can be determined.

3.3 Simulation of Stationary Motions with the Unconditioned Approach

Let $k = 1, \ldots, n$ denote the index of a target site with frequency-response functions $H_k(\omega)$ and let $\gamma_{kl}(\omega)$ denote the coherency function describing the variability of the motions between two sites k and l. Let $\mathbf{X}_p = [\, A_{p1} \quad B_{p1} \quad \ldots \quad A_{pn} \quad B_{pn} \,]$ denote the set of Fourier coefficients at frequency ω_p and let $\mathbf{\Sigma}_{pp}$ denote the $2n \times 2n$ covariance matrix of these coefficients. The covariance matrix fully defines the zero-mean joint Gaussian distribution of vector $\mathbf{X}_p$. The elements $\mathbf{\Sigma}_{pp,ij}$ of this matrix are determined using Eqs. 10 and 11. The latter equations involve the auto-PSDs $G_{kk}\left(\omega_p\right)$, $k = 1, \ldots, n$, and the cross-PSDs $G_{kl}\left(\omega_p\right)$, $k, l = 1, \ldots, n$, $k \neq l$. To determine the auto-PSDs, first, the auto-PSD of the given realization is estimated through the (optionally smoothed) periodogram given in Eq. 6. In the sequel, the full set of auto-PSDs is obtained in terms of the estimated auto-PSD of the given realization and the site frequency-response functions, using the relation between the PSDs of the surface motions at two locations k and l:

$$G_{ll}(\omega) = G_{kk}(\omega)\,\frac{|H_l(\omega)|^2}{|H_k(\omega)|^2} \tag{12}$$

The above equation is based on the same assumptions as those behind Eq. 4. The full set of cross-PSDs can then be obtained in terms of the auto-PSDs and the given coherency function (see Eq. 1).

Once the covariance matrix is determined, sample vectors from the $2n$-dimensional zero-mean joint Gaussian distribution of $\mathbf{X}_p$ are obtained as $\mathbf{x}_p = \mathbf{L}_p^{\mathrm{T}}\mathbf{z}_p$, where $\mathbf{L}_p$ is an upper triangular matrix such that $\mathbf{L}_p^{\mathrm{T}}\mathbf{L}_p = \Sigma_{pp}$ and $\mathbf{z}_p$ is a $2n$-vector of uncorrelated standard normal variables. A computationally efficient method to obtain $\mathbf{L}_p$ is to write it as $\mathbf{L}_p = \mathbf{D}_p\mathbf{R}_p$, where $\mathbf{D}_p$ is the diagonal matrix of standard deviations and $\mathbf{R}_p$ is the Cholesky decomposition of the correlation matrix.

After sampling at all frequencies $\omega_p = 2\pi p/N\Delta t$, $p = 0, 1, \ldots, N/2$, Eq. 9 is used to obtain the acceleration time-histories at the n sites. Note that the ground motions are fully coherent at $\omega_p = 0$ and the Fourier coefficients have the same values at all locations. Thus, at $\omega_p = 0$, one only needs to sample from a 1-dimensional zero-mean Gaussian distribution with variance $G_{kk}(0)\Delta\omega$.

3.4 Simulation of Stationary Motions with the Conditioned Approach

In the current approach, the Fourier coefficients of the acceleration processes at the target locations are sampled from a joint Gaussian distribution derived by probabilistic conditioning. Consider again the vector of zero-mean Fourier coefficients $\mathbf{X}_p = [\, A_{p1} \quad B_{p1} \quad \ldots \quad A_{pn} \quad B_{pn} \,]$ at frequency ω_p, and the $2n \times 2n$ covariance matrix $\mathbf{\Sigma}_{pp}$ of these coefficients. The vector $\mathbf{X}_p$ is partitioned into two subvectors, $\mathbf{X}_{p1}$ and $\mathbf{X}_{p2}$, with the former including the Fourier coefficients at sites with known ground motions. The conditional distribution of $\mathbf{X}_{p2}$ given $\mathbf{X}_{p1} = \mathbf{x}_{p1}$ is jointly normal with mean:

$$\mathbf{M}_{p,21} = \mathbf{\Sigma}_{pp,21}\left(\mathbf{\Sigma}_{pp,11}\right)^{-1}\mathbf{x}_{p1} \tag{13}$$

and covariance matrix:

$$\mathbf{\Sigma}_{p,22\,11} = \mathbf{\Sigma}_{pp,22} - \mathbf{\Sigma}_{pp,21}\left(\mathbf{\Sigma}_{pp,11}\right)^{-1}\mathbf{\Sigma}_{pp,12} \tag{14}$$

where $\mathbf{\Sigma}_{pp,ij}$ denotes the sub-matrix of $\mathbf{\Sigma}_{pp}$ giving the covariance of vectors $\mathbf{X}_{pi}$ and $\mathbf{X}_{pj}$. The covariance matrix $\mathbf{\Sigma}_{pp}$, is obtained as described in the previous subsection.

The case when the acceleration process is specified at location $k = 1$ only is herein considered. Accordingly, conditioned acceleration time-histories are simulated for locations $k = 2, \ldots, n$. The $2(n-1)$-dimensional joint Gaussian distribution of the Fourier coefficients for the target $n-1$ locations is defined through the conditional mean vector and covariance matrix in Eqs. 13 and 14 respectively. In these equations, $\mathbf{x}_{p1} = [\, A_{p1} \quad B_{p1} \,]$ is the set of Fourier coefficients of the given accelerogram. At each frequency $\omega_p = 2\pi p/N\Delta\mathrm{t}$, $p = 1, \ldots, N/2$, a sample-set of Fourier coefficients for the target locations is obtained as $\mathbf{x}_{p2} = \mathbf{M}_{p,2|1} + \mathbf{L}^{\mathrm{T}}_{p,2|1}\mathbf{z}_p$, where $\mathbf{L}_{p,2\,1}$ is an upper triangular matrix such that $\mathbf{L}^{\mathrm{T}}_{p,2|1}\mathbf{L}_{p,2|1} = \mathbf{\Sigma}_{pp,22|11}$, and $\mathbf{z}_p$ is a $2(n-1)$-vector of uncorrelated standard normal variables. Sampling is not required for $p = 0$, because at $\omega_p = 0$ the ground motions are fully coherent and the Fourier coefficients have the same values at all locations. After the vectors $\mathbf{x}_{p2}$ at all frequencies are obtained, Eq. 9 is used to assemble the realizations of acceleration time-histories at the target locations.

3.5 Extension to Non-stationary Motions

As explained earlier, typical earthquake accelerograms that do not contain a directivity pulse can be seen as consisting of nearly-stationary segments. The segments should be defined so that they maintain nearly time-invariant statistical characteristics, i.e. variance, predominant frequency and bandwidth, respectively measured in terms of the integral of the squared acceleration in time, the cumulative count of zero-level up-crossings and the cumulative count of negative maxima or positive minima (see also the subsection on estimation of the coherency modulus).

The basic idea of the non-stationary extension of the unconditioned simulation is to apply the method described earlier to each "stationary" segment of the given accelerogram and then, for each location, assemble the entire realization by joining together the corresponding simulated segments. Following the segmentation of the given accelerogram, both ends of each segment need to be tapered with appropriate (e.g. cosine-type) functions so as not to introduce fake high-frequency components in the Fourier series. To avoid shifting the segments for different sites, the wave-passage effect is separately applied as a deterministic time-shift on the entire realization. Finally, the shifted accelerograms are further processed following standard techniques in earthquake engineering, i.e. subtraction of the mean value of the entire acceleration time-history, application of a short cosine taper function to set the initial value to zero and application of a high-pass filter to ensure zero residual velocity and displacement. The resulting acceleration time-histories are integrated to obtain the corresponding velocity and displacement realizations.

The non-stationary extension of the conditioned simulation method is performed in a manner similar to that described above for the unconditioned simulation. However, in order to obtain a consistent set of ground motions, the given accelerogram at the reference site must be slightly modified by joining together the tapered segments and post-processing the entire time-history in a manner identical to the simulated motions. The resulting motion at the reference site does not have any random characteristics but is slightly different from the given record. The segmentation and post-processing mainly influence the low-frequency content of the motion, which is more apparent in the displacement waveform. As a result, the displacement time-history of the original record may somewhat differ from the simulated displacement time-history at zero distance. If accurate representation of the displacement time-history of the original record is important, the following alternative procedure can be applied: (a) the low-frequency component of the original record is separated, e.g. by use of a high-pass filter; (b) conditioned non-stationary motions are simulated based on the remaining component; (c) the low-frequency component is added back to the simulated time-histories after it has been deterministically modified to account for the wave-passage effect and, optionally, for the site-response effect.

3.6 Example Application

An example application from Konakli and Der Kiureghian (2012a) is herein presented in brief. Support motions are simulated for an example four-span bridge in California with its five supports located at sites with varying soil conditions. The five supports comprise abutment 1, bent 2, bent 3, bent 4 and abutment 5. The acclererogram at the reference site (abutment 1) is the fault-normal component of the Izmit record from the 1999 Kocaeli earthquake. For further details on the bridge configuration and the characteristics of the ground motion random field, the reader is referred to Konakli and Der Kiureghian (2012a).

Figure 4 shows example sets of support motions generated with the unconditioned and conditioned approaches (left and right graphs respectively). For each example simulation, acceleration, velocity and displacement time-histories at the five supports are shown. Note that both simulation approaches preserve the non-stationary nature of the ground motion and that all records approach zero with increasing time. The motions in the pair of abutments 1 and 5 and the pair of bents 2 and 4 differ only due to incoherence and wave passage, and thus, have the same frequency contents. For any other pair of support motions, the variability is additionally due to the effect of varying soil conditions. These differences in the frequency contents are more apparent in the acceleration than in the velocity and displacement time-histories, with the lower frequency contents indicating softer sites.

Figure 5 shows 5% damped pseudo-acceleration response spectra at each support point for 20 realizations obtained from unconditioned and conditioned simulations (left and right graphs respectively). For the unconditioned case, the variances at all support points are similar, which, as explained before, is a desirable characteristic for ground motions to be used in statistical analyses of structural responses. For the conditioned case, one notes the increasing variance of the spectral amplitude with increasing distance from abutment 1, at which the variance is zero.

Figure 6 compares the acceleration coherency estimates from the simulated motions with the corresponding target theoretical models for an example pair of support points (abutment 1 and bent 3). The real and imaginary parts of the coherency function are shown in the upper and bottom graphs respectively. The coherency estimates are obtained by averaging the estimates from 20 realizations. Excellent agreement of the coherency estimates with the theoretical model validates the accuracy of both the unconditioned and the conditioned approaches (see left and right graphs of the figure respectively). It is noted that an equally good agreement of the estimated coherency with the target theoretical models has also been verified for the other pairs of supports.

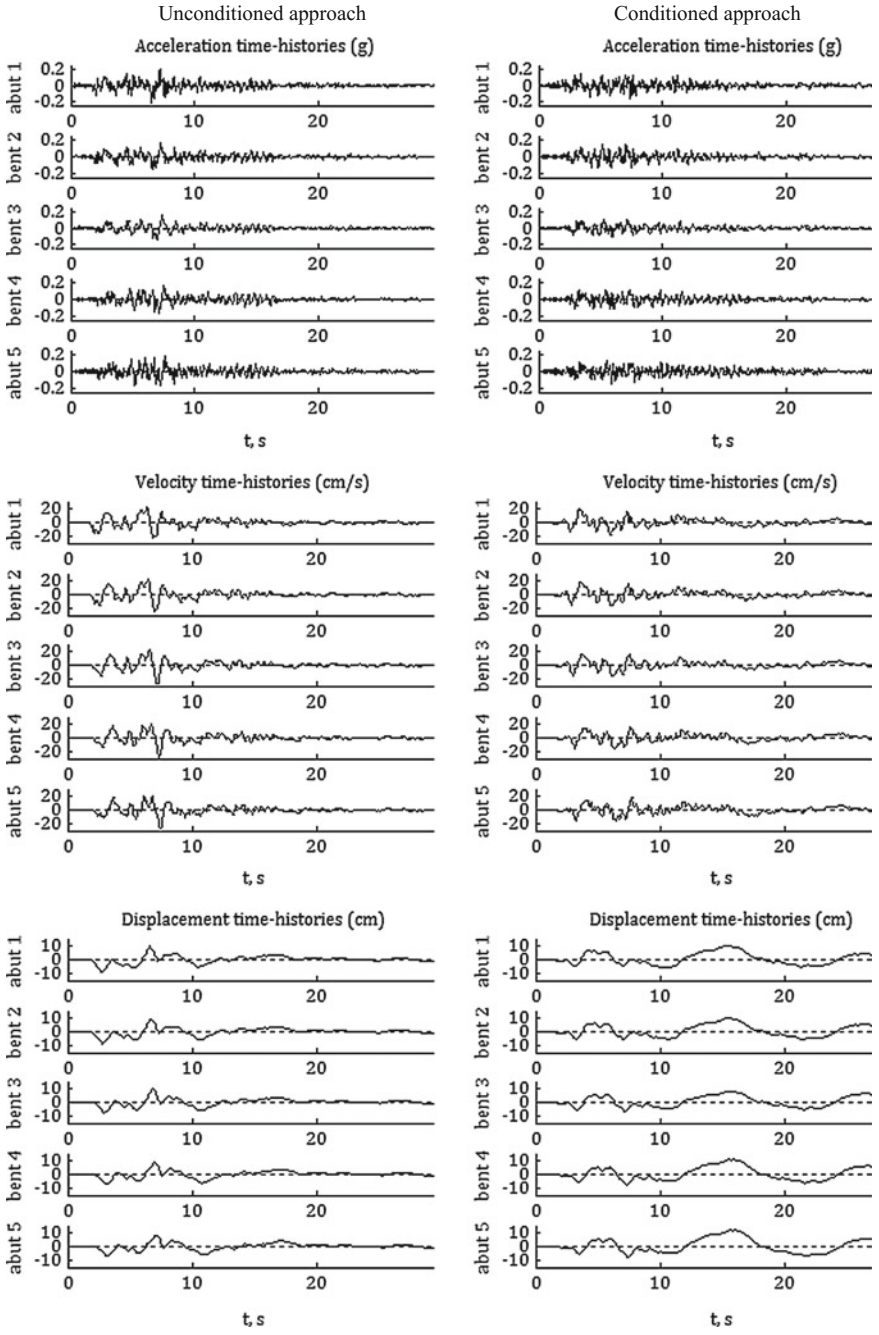

Fig. 4 Example sets of simulated support motions

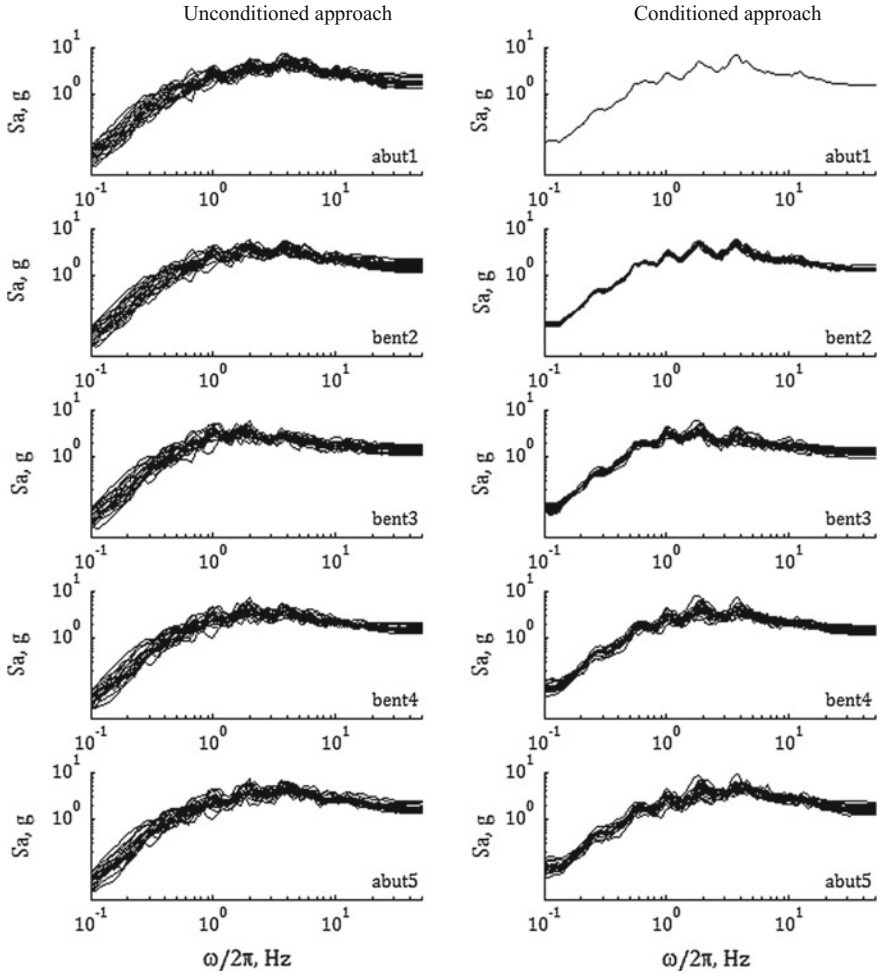

Fig. 5 Pseudo-acceleration response spectra for 20 simulated arrays

4 Structural Response to Differential Support Excitation

4.1 Linear Response Analysis with Response-Spectrum Methods

Analysis of structural response to differential support excitations can be performed using time-history analysis (e.g. Saxena et al. 2000; Sextos et al. 2004; Lou and Zerva 2005; Lupoi et al. 2005) the methods of random vibration (e.g. Dumanogluid and Soyluk 2003; Zembaty and Rutenberg 2002; Zhang et al. 2009; Heredia-Zavoni et al. 2015) or response spectrum methods (e.g. Berrah and Kausel 1992;

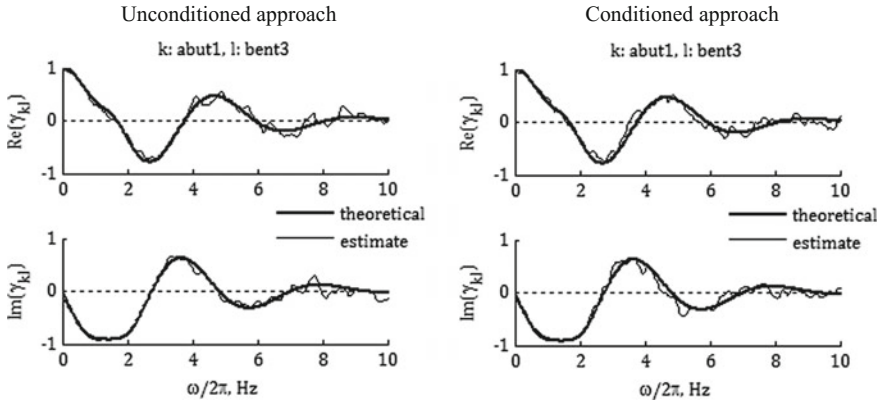

Fig. 6 Acceleration coherency estimates from 20 simulated arrays

Der Kiureghian and Neuenhofer 1992; Konakli and Der Kiureghian 2011a). The random vibration and response spectrum approaches provide a statistical characterization of the response and therefore, their results are not specific to a particular set of ground motions. In this respect, the aforementioned two approaches are deemed advantageous to time-history analysis. Due to the simplicity of characterizing ground motions with response spectra, the response-spectrum approach is particularly appealing in engineering practice.

The Multiple-Support Response-Spectrum (MSRS) rule, developed by Der Kiureghian and Neuenhofer (1992), evaluates the mean peak response of multiply-supported linear structures subjected to spatially varying ground motions. This rule has become a popular method of analysis of multiply-supported structures (see, e.g. Kahan et al. 1996; Soyluk 2004; Wang and Chen 2005; Yu and Zhou 2008; Wang and Der Kiureghian 2014) and is also incorporated by seismic codes (Eurocode 8 1998). The original formulation of this method only considered responses that could be expressed as linear functions of the total displacements at unconstrained degrees of freedom (DOF) of the structure. Konakli and Der Kiureghian (2011a) generalized the original formulation to account for response quantities that also depend on the support motions. Such dependence is pervasive among response quantities of interest; for instance, when rotational DOF are condensed out in the analysis, most response quantities of interest indirectly depend on the support motions. Konakli and Der Kiureghian (2011a) further developed an extended version of the MSRS rule that accounts for quasi-static contribution of truncated high-frequency modes. This extension is particularly important in engineering practice, where computational costs necessitate the truncation of modes beyond a number far smaller than the total number of DOF of the structure. The generalized and extended MRSS rules are described in the sequel.

4.2 The Generalized MSRS Rule

Consider a linear structural system with N unconstrained DOF and subjected to m support motions. Let $\mathbf{x} = [\, x_1 \quad \ldots \quad x_N \,]^{\mathrm{T}}$ denote the N-vector of (total) displacements at the unconstrained DOF and $\mathbf{u} = [\, u_1 \quad \ldots \quad u_m \,]^{\mathrm{T}}$ denote the m-vector of prescribed support displacements. Assuming classical damping, let $\mathbf{\Phi} = [\, \mathbf{\Phi}_1 \quad \ldots \quad \mathbf{\Phi}_N \,]$, ω_i and, ζ_i, $i = 1, \ldots, N$, respectively denote the modal matrix, natural frequencies, and modal damping ratios of the fixed-base structure. Moreover, let $s_{ki}(t)$ denote the normalized response of the ith mode to the kth support motion, obtained as the solution to:

$$\ddot{s}_{ki}(t) + 2\zeta_i \omega_i \dot{s}_{ki}(t) + \omega_i^2 s_{ki}(t) = -\ddot{u}_k(t) \tag{15}$$

A generic response quantity of interest $z(t)$ can be written as a linear combination of the support displacements and the displacements at the unconstrained DOF:

$$z(t) = \mathbf{q}_u^T \mathbf{u}(t) + \mathbf{q}_x^T \mathbf{x}(t) \tag{16}$$

where $\mathbf{q}_u = [\, q_{u,1} \quad \ldots \quad q_{u,m} \,]^{\mathrm{T}}$ and $\mathbf{q}_x = [\, q_{x,1} \quad \ldots \quad q_{x,N} \,]^{\mathrm{T}}$ are coefficient vectors. Equation 16 represents a generalization of the original formulation by Der Kiureghian and Neuenhofer (1992), who considered $z(t)$ a function of $\mathbf{x}(t)$ only. This generalization allows consideration of response quantities that are functions of displacements at both the constrained as well as support DOF, e.g. the drift of a bridge column or an internal force of a structural model with condensed rotational DOF.

Based on principles of modal analysis, Eq. 16 can be written as (Konakli and Der Kiureghian 2011a):

$$z(t) = \sum_{k=1}^{m} a_k u_k(t) + \sum_{k=1}^{m} \sum_{i=1}^{N} b_{ki} s_{ki}(t) \tag{17}$$

where a_k represents the response quantity of interest when the kth support DOF is statically displaced by a unit amount while all other support DOF remaining fixed, and b_{ki} represents the contribution of the ith mode to the response arising from the excitation at the kth support DOF when the normalized modal response $s_{ki}(t)$ is equal to unity. The coefficients a_k and b_{ki} are given by:

$$a_k = q_{u,k} + \mathbf{q}_x^T \mathbf{r}_k \tag{18}$$

where $\mathbf{r}_k$ represents the displacements at the unconstrained DOF when the kth support DOF is displaced by a unit amount, and:

$$b_{ki} = \mathbf{q}_x^T \boldsymbol{\Phi}_i \beta_{ki} \tag{19}$$

where $\beta_{ki} = \boldsymbol{\Phi}_i^{\mathrm{T}} \mathbf{M}\mathbf{r}_k / \boldsymbol{\Phi}_i^{\mathrm{T}} \mathbf{M} \boldsymbol{\Phi}_i$ is the modal participation factor associated with the ith mode and kth support DOF; in the latter expression, $\mathbf{M}$ denotes the mass matrix of the structure associated with the unconstrained DOF. The coefficients a_k and b_{ki} depend only on the structural properties and can be computed by use of any conventional static analysis program (see Konakli and Der Kiureghian 2011a, b, for further details on properties of these coefficients and their computation).

Using Eq. 17 and the principles of stationary random vibration theory, the mean of the peak of the generic response quantity $z(t)$ can be approximately obtained in the form (Der Kiureghian and Neuenhofer 1992):

$$\begin{aligned} &E[\max|z(t)|] \\ &\approx \Bigg[\sum_{k=1}^{m} \sum_{l=1}^{m} a_k a_l \rho_{u_k u_l} u_{k,max} u_{l,max} \\ &+ 2 \sum_{k=1}^{m} \sum_{l=1}^{m} \sum_{j=1}^{N} a_k b_{lj} \rho_{u_k s_{lj}} u_{k,max} D_l(\omega_j, \zeta_j) \\ &+ \sum_{k=1}^{m} \sum_{l=1}^{m} \sum_{i=1}^{N} \sum_{j=1}^{N} b_{ki} b_{lj} \rho_{s_{ki} s_{lj}} D_k(\omega_i, \zeta_i) D_l(\omega_j, \zeta_j) \Bigg]^{1/2} \end{aligned} \tag{20}$$

The preceding equation represents the MSRS combination rule. The mean of the peak response is given in terms of: (i) the structural properties, reflected in the coefficients a_k and b_{ki}, (ii) the mean peak ground displacements $u_{k,\max}$ and the ordinates of the mean displacement response spectra $D_k(\omega_i, \zeta_i)$, and (iii) three sets of correlation coefficients. The latter comprise the coefficients $\rho_{u_k u_l}$, describing the correlation between the kth and lth support displacements, the coefficients $\rho_{u_k s_{lj}}$, describing the correlation between the kth support displacement and the response of the jth mode to the lth support motion, and the coefficients $\rho_{s_{ki} s_{lj}}$, describing the correlation between the responses of the ith and jth modes to the kth and lth support motions respectively.

The correlation coefficient for two processes $x(t)$ and $y(t)$ is defined as:

$$\rho_{xy} = \frac{\int_{-\infty}^{+\infty} G_{xy}(\omega) d\omega}{\left[\int_{-\infty}^{+\infty} G_{xx}(\omega) d\omega \int_{-\infty}^{+\infty} G_{yy}(\omega) d\omega\right]^{1/2}} \tag{21}$$

where $G_{xx}(\omega)$ is the auto-PSD of $x(t)$, and $G_{xy}(\omega) = \gamma_{xy}(\omega)[G_{xx}(\omega) G_{yy}(\omega)]^{1/2}$ is the cross-PSD of $x(t)$ and $y(t)$, with $\gamma_{xy}(\omega)$ denoting the coherency function. The processes involved in the computation of the correlation coefficients of the MSRS rule are the support displacements $u_k(t)$ and the normalized modal responses $s_{ki}(t)$. The auto-PSD of $u_k(t)$ can be obtained in terms of the response spectrum $D_k(\omega, \zeta)$, while the auto-PSD of $s_{ki}(t)$ additionally involves the frequency-response function

of the *i*th mode (see Der Kiureghian and Neuenhofer 1992, for details). It follows that the complete set of correlation coefficients can be obtained in terms of the response spectra at the support DOF, the coherency function and the modal properties of the structure.

Konakli and Der Kiureghian (2012b) investigated the accuracy of the MSRS rule by comparing the MSRS estimates of mean peak structural responses with the corresponding 'exact' mean values obtained by time-history analysis. The considered structural systems comprised four bridge models designed by the California Department of Transportation and characterized by distinctly different configurations and dynamic properties. The focus of the study was set on pier drifts, which are quantities particularly important in performance-based design of bridges. The analysis assumed uniform soil conditions, but incorporated effects of incoherence and wave passage. Support-motion arrays for the time-history analysis were obtained with the unconditioned simulation method, described in the previous section. The study considered two recorded accelerograms as seeds in the simulation of the support motions and two levels of incoherence. For each ground motion random field, 20 ensembles of ground-motions arrays were generated. The mean response spectra of the motions at all supports of a bridge were used as input in the MSRS analysis.

As an example, Fig. 7 shows the time histories of three pier drifts (from different bridges) for a particular ground-motion random field (20 realizations) together with the corresponding MSRS estimates, the latter depicted by horizontal lines. Examining absolute values of the MSRS errors, the mean and standard deviation over all pier drifts and ground-motion random fields considered were found equal to 4.6% and 3.7% respectively. The maximum error observed was 12.3%, but in most cases, the errors were smaller than 10%.

It is emphasized that the MSRS method is intended for use in conjunction with smooth response spectra that represent broadband excitations and a smooth coherency function. In the aforementioned analysis however, jagged response spectra from relatively narrowband excitations were used. Furthermore, the smooth coherency function used for evaluation of the correlation coefficients in the MSRS analysis differs from the actual coherency values for pairs of simulated support motions, which may exhibit fluctuations around the theoretical model. In view of these differences, the reported MSRS errors are deemed remarkably small.

4.3 The Extended MSRS Rule

When high-frequency modes are truncated, an improved approximation of the response can be obtained by accounting for the quasi-static contributions of the truncated modes. If ω_i is large relative to the frequencies of the input excitation, the last term in the left-hand side of Eq. 15 is dominant and the *i*th normalized

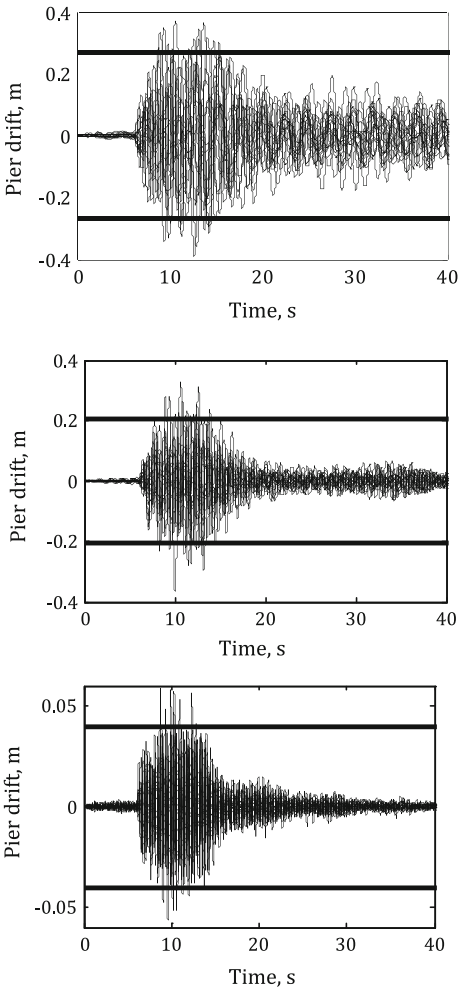

Fig. 7 Response time-histories and corresponding MSRS estimates

modal response to the kth support motion can be approximated by $s_{ki}(t) \approx -\omega_i^{-2}\ddot{u}_k(t)$. Using this relation in Eq. 17 for modes $i > n$ leads to:

$$z(t) \approx \sum_{k=1}^{m} a_k u_k(t) + \sum_{k=1}^{m}\left[\sum_{i=1}^{n} b_{ki} s_{ki}(t) - \sum_{i=n+1}^{N} \frac{b_{ki}}{\omega_i^2}\ddot{u}_k(t)\right] \tag{22}$$

The coefficients b_{ki} for $i > n$ can be eliminated from Eq. 22 by employing the identity (Konakli and Der Kiureghian 2011a):

$$-\sum_{i=1}^{N}\frac{b_{ki}}{\omega_i^2}=-\mathbf{q}_x^T\mathbf{K}^{-1}\mathbf{M}\mathbf{r}_k \tag{23}$$

where $\mathbf{K}$ denotes the stiffness matrix of the structure associated with the unconstrained DOF. By rearranging terms, one obtains:

$$\sum_{i=n+1}^{N}\frac{b_{ki}}{\omega_i^2}=\mathbf{q}_x^T\mathbf{K}^{-1}\mathbf{M}\mathbf{r}_k-\sum_{i=1}^{n}\frac{b_{ki}}{\omega_i^2}=d_k \tag{24}$$

Using the above identity, Eq. 22 can be written in a form that involves the dynamic properties of only the first n modes:

$$z(t)\approx\sum_{k=1}^{m}a_k u_k(t)+\sum_{k=1}^{m}\sum_{i=1}^{n}b_{ki}s_{ki}(t)-\sum_{k=1}^{m}d_k\ddot{u}_k(t) \tag{25}$$

Note that this improved expression of the response additionally involves the support accelerations $\ddot{u}_k(t)$.

Based on Eq. 25 and principles of random vibration theory, the extended MSRS rule that accounts for contributions of truncated modes is obtained as:

$$\begin{aligned}
&E[max|z(t)|]\\
&\approx\Bigg[\sum_{k=1}^{m}\sum_{l=1}^{m}a_k a_l\rho_{u_k u_l}u_{k,max}u_{l,max}\\
&+2\sum_{k=1}^{m}\sum_{l=1}^{m}\sum_{j=1}^{n}a_k b_{lj}\rho_{u_k s_{lj}}u_{k,max}D_l(\omega_j,\zeta_j)\\
&+\sum_{k=1}^{m}\sum_{l=1}^{m}\sum_{i=1}^{n}\sum_{j=1}^{n}b_{ki}b_{lj}\rho_{s_{ki}s_{lj}}D_k(\omega_i,\zeta_i)D_l(\omega_j,\zeta_j)\\
&+\sum_{k=1}^{m}\sum_{l=1}^{m}d_k d_l\rho_{\ddot{u}_k\ddot{u}_l}\ddot{u}_{k,max}\ddot{u}_{l,max}-2\sum_{k=1}^{m}\sum_{l=1}^{m}\rho_{u_k\ddot{u}_l}u_{k,max}\ddot{u}_{l,max}\\
&-2\sum_{k=1}^{m}\sum_{l=1}^{m}\sum_{i=1}^{n}b_{ki}d_l\rho_{s_{ki}\ddot{u}_l}D_k(\omega_i,\zeta_i)\ddot{u}_{l,max}\Bigg]^{1/2}
\end{aligned} \tag{26}$$

The extended MSRS rule adds the last three terms to the original formulation. The first of these terms represents the static contribution of the truncated modes. The second term arises from the covariances of the support displacements and accelerations, while the last term arises from the covariances between the responses of the included modes and the static responses of the truncated modes. These terms involve the peak support accelerations and three sets of correlation coefficients. The new coefficients $\rho_{\ddot{u}_k\ddot{u}_l}$, $\rho_{u_k\ddot{u}_l}$ and $\rho_{s_{ki}\ddot{u}_l}$ respectively describe: the correlation between the ground accelerations at the kth and lth support DOF, the correlation between the ground displacement at the kth support DOF and the ground acceleration at the lth support DOF, and the correlation between the ith modal response to the excitation

at the kth support DOF and the ground acceleration at the lth support DOF. The accuracy of the MSRS coefficients $\rho_{u_k u_l}$, $\rho_{\ddot{u}_k \ddot{u}_l}$ and $\rho_{u_k \ddot{u}_l}$ (the last two appearing only in the extended rule) was examined by Konakli (2013).

For an assessment of the improvement obtained with the extended rule, the interested reader is referred to Konakli and Der Kiureghian (2011a).

4.4 Non-linear Response: The 'Equal Displacement' Rule

Non-linear response-history analysis (RHA) represents the most accurate method for the evaluation of inelastic structural response to a specified set of support motions. However, non-linear RHA faces two important constraints: (i) it is computationally costly and (ii) by providing results that are particular to the selected input time-histories, it has limited ability to characterize effects of uncertainties that surround future ground motions. Although response-spectrum methods overcome these limitations, they are restricted to linear response analysis. It is thus of interest to investigate relations between non-linear responses and their linear counterparts.

Observations by Veletsos and Newmark (1960) on the responses of elasto-plastic and the corresponding linear single-DOF systems gave rise to the 'equal displacement' rule. Under certain conditions, this rule allows estimation of the maximum displacement response of inelastic structures from analysis of their elastic counterparts. The 'equal displacement' rule is particularly useful in displacement-based design procedures (Moehle 1992, Kowalsky 2002), which are of growing interest in performance-based earthquake engineering. Therefore, several studies have been devoted to assessing its accuracy and limitations for different types of structures and ground motions. The applicability of the 'equal displacement' rule for extended structures subjected to differential support motions was investigated by Konakli and Der Kiureghian (2014); a brief description of the analysis and main findings of this study is given next.

Konakli and Der Kiureghian (2014) compared responses from linear and non-linear time-history analyses for idealized models of four actual bridges in California with distinctly different configuration and dynamic properties. They performed statistical analyses of the maximum pier drifts for ground-motion random fields with different frequency contents and spatial variability characteristics. In particular, the analysis considered two seed recorded accelerograms and four cases of spatial variability:

- Case 1 represents uniform support excitations.
- Case 2 incorporates effects of incoherence and wave passage, but assumes uniform soil conditions.
- Case 3 differs from case 2 in considering a higher level of incoherence.
- Case 4 differs from case 2 in assuming varying soil profiles.

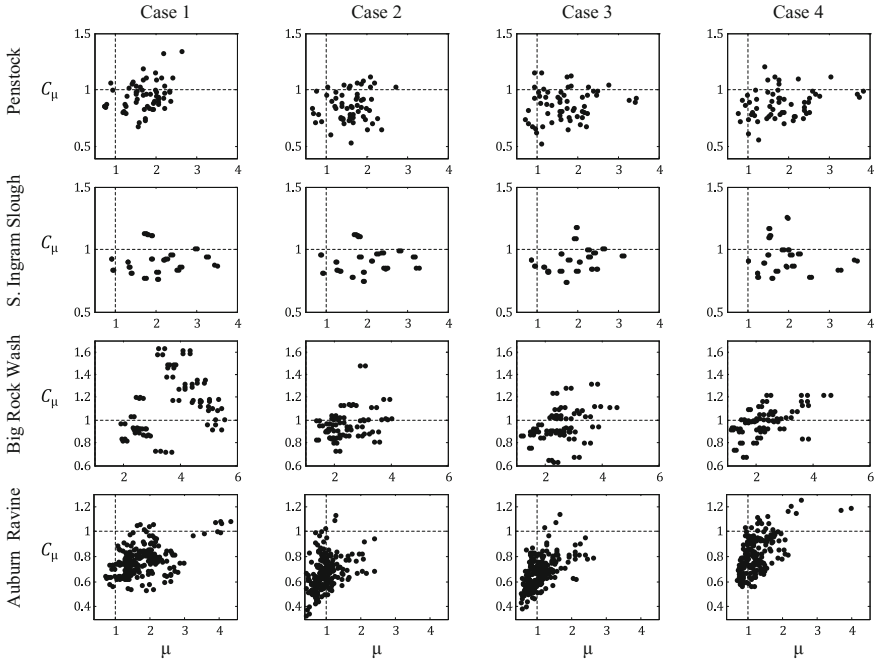

Fig. 8 Inelasticity versus ductility factors

As ensemble of 20 support-motion arrays were simulated for each bridge model and ground-motion random field. Based on the respective pier-drift responses from linear and non-linear RHA, Konakli and Der Kiureghian (2014) analyzed the statistics of two dimensionless response quantities: (i) the ductility factor μ, representing the ratio of peak pier drift from non-linear RHA to the corresponding yield drift, and (ii) the inelasticity factor C_μ, representing the ratio of peak non-linear to peak linear drift. Graphs of inelasticity versus ductility factors for one seed accelerogram are shown in Fig. 8, where graphs in the same row correspond to a single bridge model, whereas graphs in the same column correspond to a certain case of spatial variability.

Under uniform support motions (case 1) and for moderate levels of inelastic behavior, the 'equal displacement' rule was found fairly accurate for cases when the fundamental period of the bridge was beyond the acceleration-controlled range of the response spectrum. For bridges with shorter fundamental periods, the rule was found non-conservative for cases with mean ductility factors in the range from 3 to 4 and overly conservative for cases with mean ductility factors smaller than approximately 2. Wave passage and incoherence (cases 2 and 3) reduced the mean inelasticity factors, but the latter increased when the effect of differential site response was additionally incorporated by locating piers on softer soils (case 4). Effects of spatial variability on the pier-drift response were more pronounced for

longer and stiffer bridges. In most cases, mild or moderate positive linear correlations between inelasticity and ductility factors were observed, with the higher correlations observed for bridges with fundamental periods shorter than the transition period between the acceleration- and velocity-controlled ranges of the response spectrum.

5 Conclusions and Perspectives

This chapter provided an overview on methods for incorporating effects of ground-motion spatial variability in seismic response assessment, based on concepts of stochastic time-series analysis and random vibration theory. The examined topics included the modeling of ground-motion spatial variability, the simulation of spatially varying ground-motion arrays and the evaluation of structural response to differential support motions. The modeling of the ground-motion spatial variability relied on the coherency function; the different elements of this function as well as its estimation based on recorded motions were explained. The presented method for simulating spatially varying ground motions incorporates the incoherence, wave-passage and site-response effects and preserves the temporal and spectral non-stationarity of a specified reference accelerogram. In particular, the unconditioned simulation approach yields arrays with uniform variability that can be used as input for the statistical analysis of structural response. The Multiple-Support Response-Spectrum (MSRS) rule and its extended version were described as a means for obtaining a statistical characterization of the peak linear structural response. Finally, investigations into the relations between peak linear and non-linear responses under effects of ground-motion spatial variability provided insights into the validity of the 'equal displacement' rule in this case of excitation.

Inspired by the particular case of seismic response analysis to correlated support motions, this chapter closes with the hope that methods of stochastic analysis will be more widely employed in engineering practice, as a valuable tool for dealing with the significant uncertainties facing engineering design. The importance of a systemic perspective that properly accounts for the pertinent inter-dependencies and correlations is also emphasized. The most modern research findings in the aforementioned areas can be effectively transferred into engineering practice through the continuing education of engineers, the interactions between research and practice and the systematic research-informed updating of the engineering codes.

Acknowledgements I would like to express my deep gratitude to Professor Armen Der Kiureghian for his excellent academic advising and the invaluable support and encouragement he provided to me not only during my doctoral years, but also in the pursuit of my dreams thereafter. His personality, values and accomplishments are a unique source of inspiration. I have the honor of keeping one of his paintings, depicting the Bay Bridge in San Francisco, a reminder of my very meaningful graduate years at Berkeley that opened up new wonderful horizons in my life.

References

Abrahamson NA, Schneider JF, Stepp JC (1991) Empirical spatial coherency functions for application to soil-structure interaction analyses. Earthq Spectra 7:1–28

Ancheta TD, Stewart JP, Abrahamson NA (2011) Engineering characterization of earthquake ground motion coherency and amplitude variability. In: Earthquake engineering, UCLA civil and environmental engineering, UC Los Angeles

Berrah M, Kausel E (1992) Response spectrum analysis of structures subjected to spatially varying motions. Earthq Eng Struct Dyn 21:461–470

Brillinger RD (2001) Time series: data analysis and theory. Soc Ind Appl Math

Chatfield C (2004) The analysis of time series: an introduction, 6th edn. CRC Press LLC

Der Kiureghian A (1996) A coherency model for spatially varying ground motions. Earthq Eng Struct Dyn 25:99–111

Der Kiureghian A, Ke JB (1988) The stochastic finite element method in structural reliability. Probab Eng Mech 3:83–91

Der Kiureghian A, Liu PL (1986) Structural reliability under incomplete probability information. J Eng Mech 112:85–104

Der Kiureghian A, Neuenhofer A (1992) Response spectrum method for multiple-support seismic excitation. Earthq Eng Struct Dyn 21:713–740

Der Kiureghian A, Zhang Y, Li CC (1994) Inverse reliability problem. J Eng Mech 120: 1154–1159

Dumanogluid A, Soyluk K (2003) A stochastic analysis of long span structures subjected to spatially varying ground motions including the site-response effect. Eng Struct 25:1301–1310

Eurocode 8: Design of structures for earthquake resistance-part 2: bridges (1998)

Harichandran RS, Vanmarcke EH (1986) Stochastic variation of earthquake ground motion in space and time. J Eng Mech 112:154–174

Heredia-Zavoni E, Santa-Cruz S, Silva-González FL (2015) Modal response analysis of multi-support structures using a random vibration approach. Earthq Eng Struct Dyn 44(13):2241–2260

Kahan M, Gibert RJ, Bard PY (1996) Influence of seismic waves spatial variability on bridges: a sensitivity analysis. Earthq Eng Struct Dyn 25:795–814

Kameda H, Morikawa H (1992) An interpolating stochastic process for simulation of conditional random fields. Probab Eng Mech 7:243–254

Konakli K, Der Kiureghian A (2011a) Extended MSRS rule for seismic analysis of bridges subjected to differential support motions. Earthq Eng Struct Dyn 40:1315–1335

Konakli K, Der Kiureghian A (2011b) Stochastic dynamic analysis of bridges subjected to spatially varying ground motions. Report No. 2011/105, Pacific earthquake engineering research center, University of California, Berkeley

Konakli K, Der Kiureghian A (2012a) Simulation of spatially varying ground motions including incoherence, wave-passage and differential site-response effects. Earthq Eng Struct Dyn 41:495–513

Konakli K, Der Kiureghian A (2012b) Evaluation of the accuracy of the Multiple Support Response Spectrum (MSRS) method. In: Proceedings of 15th world conference on earthquake engineering, Lisbon, Portugal

Konakli K (2013) Spatial correlations in seismic response analysis of extended structures. In: 11th international conference on structural safety and reliability, Columbia University, New York

Konakli K, Der Kiureghian A (2014) Investigation of 'equal displacement' rule for bridges subjected to differential support motions. Earthq Eng Struct Dyn 43(1):23–39

Konakli K, Der Kiureghian A, Dreger D (2014) Coherency analysis of the UPSAR array of accelerograms recorded during the 2004 Parkfield earthquake. Earthq Eng Struct Dyn 43 (5):641–659

Kowalsky MJ (2002) A displacement-based approach for the seismic design of continuous concrete bridges. Earthq Eng Struct Dyn 31:719–747

Liao S, Zerva A (2006) Physically compliant, conditionally simulated spatially variable seismic ground motions for performance-based design. Earthq Eng Struct Dyn 35:891–919
Lou L, Zerva A (2005) Effects of spatially variable ground motions on the seismic response of a skewed, multi-span, RC highway bridge. Soil Dyn Earthq Eng 25:729–740
Luco JE, Wong HL (1986) Response of a rigid foundation to a spatially random ground motion. Earthq Eng Struct Dyn 14:891–908
Lupoi A, Franchin P, Pinto PE, Monti G (2005) Seismic design of bridges accounting for spatial variability of ground motion. Earthq Eng Struct Dyn 34:327–348
Moehle JP (1992) Displacement-based design of RC structures subjected to earthquakes. Earthq Spectra 8:403–428
Priestley MB (1981) Spectral analysis and time series. Academic Press, London
Rezaeian S, Der Kiureghian A (2008) A stochastic ground motion model with separable temporal and spectral nonstationarities. Earthquake Eng Struct Dyn 37:1565–1584
Saxena V, Deodatis G, Shinozuka M, Feng MQ (2000) Development of fragility curves for multi-span reinforced concrete bridges. In: Proceedings of the international conference on monte carlo simulation, Principality of Monaco, Austria
Sextos A, Kappos AJ, Mergos P (2004) Effect of soil-structure interaction and spatial variability of ground motion on irregular bridges: the case of the Krystallopigi Bridge. In: Proceedings of the 13th world conference on earthquake engineering, paper No. 2298, Vancouver, BC, Canada
Song J, Der Kiureghian A (2003) Bounds on system reliability by linear programming. J Eng Mech 129:627–636
Soyluk K (2004) Comparison of random vibration methods for multi-support seismic excitation analysis of long-span bridges. Eng Struct 26:1573–1583
Straub D, Der Kiureghian A (2010) Bayesian network enhanced with structural reliability methods: methodology. J Eng Mech 136:1248–1258
Vanmarcke EH, Fenton GA (1991) Conditioned simulation of local fields of earthquake ground motion. Struct Saf 10:247–264
Veletsos AS, Newmark NM (1960) Effect of inelastic behavior on the response of simple systems to earthquake motions. In: Proceedings of the 2nd world conference on earthquake engineering, Japan, vol 2, pp 895–912
Wang J, Chen H (2005) A new spatial coherence model and analytical coefficients for multi-support response spectrum combination. Earthq Eng Eng Vib 6:225–235
Wang Z, Der Kiureghian A (2014) Multiple-support response spectrum analysis using load-dependent Ritz vectors. Earthq Eng Struct Dyn 43(15):2283–2297
Yu RF, Zhou XY (2008) Response spectrum analysis for non-classically damped linear system with multiple-support excitations. Bull Earthq Eng 6:261–284
Zembaty Z, Rutenberg A (2002) Spatial response spectra and site amplification effects. Eng Struct 24:1485–1496
Zerva A, Harada T (1994) A site-specific model for the spatial incoherence of the seismic ground motions. In: Proceedings of the 5th national conference on earthquake engineering, Chicago, Illinois
Zhang YH, Li QS, Lin JH, Williams FW (2009) Random vibration analysis of long-span structures subjected to spatially varying ground motions. Soil Dyn Earthq Eng 29:620–629